ELSEVIER

Journal of Nuclear Materials 290–293 (2001) 696–700

journal of nuclear materials

www.elsevier.nl/locate/jnucmat

Plasma rotation and structure of the radial electric field in RFX

M.E. Puiatti [a,*], L. Tramontin [a], V. Antoni [a,b], R. Bartiromo [a], L. Carraro [a], D. Desideri [a,b], E. Martines [a], F. Sattin [a], P. Scarin [a], G. Serianni [a], M. Spolaore [a], M. Valisa [a], B. Zaniol [a]

[a] *Consorzio RFX, Corso Stati Uniti 4, 35127 Padova, Italy*
[b] *INFM, Unità di Padova sez. A, Padova, Italy*

Abstract

Plasma rotation has been investigated in the reversed field pinch experiment (RFX) both by spectroscopic means and by an array of Langmuir probes. The rotation velocity at the plasma edge has been deduced from the Doppler shift of the CIII emission line. The observation of other ions characterised by different radial positions, such as BIV and CV, has allowed an estimate of the velocity shear. The results of the spectroscopic measurements are in qualitative agreement with the electric probe results. Impurity and hydrogen rotation has been modified by external means and the effects on the velocity are in agreement with the induced radial electric field changes. The experimental results are interpreted by a Monte Carlo simulation and a single-fluid model.

Keywords: RFX; Electric field; Plasma flow

1. Introduction

The reversed field pinch (RFP) magnetic configuration is characterised by a high level of magnetic and electrostatic fluctuations, playing different roles at the plasma edge and in the core. The magnetic fluctuations are responsible for the particle and energy transport in the core, while the electrostatic fluctuations are believed to drive the particle transport at the edge. In tokamaks, where the particle and energy transport is associated with the electrostatic fluctuations, improved confinement is due to a highly sheared plasma flow at the edge [1]. The transport reduction may be explained by decorrelation of turbulence [2,3] or linear stabilisation of modes [4]. Also in RFPs, a high shear of the flow velocity, related to the radial electric field through the equilibrium radial force balance equation for the ith ionic species

$$E_{\mathrm{r}} = \frac{1}{n_i Z_i e} \cdot (\nabla p_i)_{\mathrm{r}} - (\mathbf{v}_i \times \mathbf{B})_{\mathrm{r}} \tag{1}$$

is associated with the confinement properties of the configuration [5,6]. In RFP's outward-directed radial electric fields have been measured in the plasma core, where the magnetic configuration is stochastic, and in the SOL, while an inward-directed E_{r} has been found right inside the last plasma surface [7]. The latter might be associated either with a non-stochastic outer region or with finite ion Larmor radius losses [8].

In this paper, Section 2 summarises the toroidal rotation measurements obtained from the Doppler shift of impurity lines and from the electric and diamagnetic drift derived by electric probes. The effect on the plasma flow of a rotating magnetic perturbation and of edge biasing is discussed in Section 3, and the results are interpreted by means of a Monte Carlo calculation and a single-fluid model (Section 4). A final summary is given in Section 5.

* Corresponding author. Tel.: +39-049 829 5032; fax: +39-049 8700 718.
E-mail address: puiatti@igi.pd.cnr.it (M.E. Puiatti).

0022-3115/01/$ - see front matter
PII: S0022-3115(00)00529-8

2. Plasma rotation

Toroidal and poloidal rotation velocities have been measured in RFX from the Doppler shift of CIII, BIV and CV spectral lines [9]. Since each of these ions is characterised by a different radial distribution, the measured velocities are to be associated with different radial shells. The profiles of the ions have been evaluated by means of a one-dimensional impurity diffusion model [10], simulating the experimental soft X-rays and line emissivities, plasma effective charge and radiated power and using the experimental density and temperature profiles and impurity influxes as input data. The toroidal velocity profile is shown in Fig. 1(a) for 600 kA discharges. The radial location associated with each ion is the average radius weighted on the emissivity along the experimental line of sight. Two different radial positions correspond to a single ion because the measurements have been performed along two different lines-of-sight. The errors on the gaussian fit of the profiles are evaluated according to [11]; typical values are given in Fig. 1(a). The toroidal rotation in the plasma core is in the direction of the plasma current, while at the edge, a rotation in the opposite direction is observed. It is worth recalling that in RFP's the poloidal magnetic field dominates over the toroidal component at the edge so that the perpendicular flow is in the toroidal direction. Comparing the results of CIII and BIV, a shear of $\sim 1.4 \times 10^5\ s^{-1}$ is obtained.

Fig. 1(b) shows the toroidal flow velocity obtained in low-current (300 kA) plasma discharges by a set of seven radially aligned electrodes, equally spaced by 8 mm,

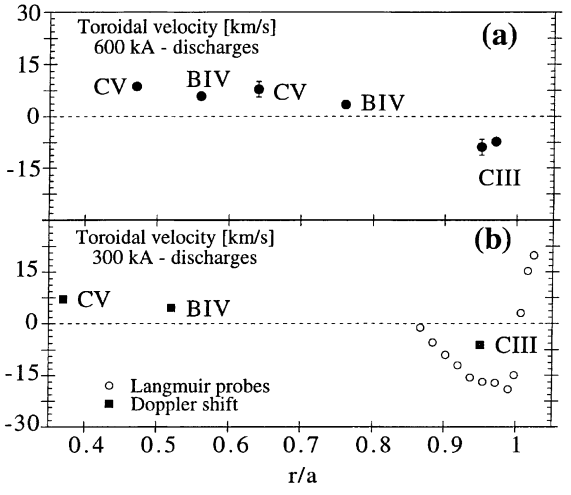

Fig. 1. (a) Toroidal flow measured from Doppler shift of CIII, BIV and CV lines in 600 kA discharges; (b) toroidal flow measured by electric probes in low plasma current discharges (300 kA) together with spectroscopic measurements (squared symbols).

each measuring the floating potential, V_f. The plasma potential, ϕ, is related to V_f and to the local electron temperature, T_e, by $\phi = V_f - \alpha T_e$, with $\alpha = -2.5$ [12]. The electric field has been approximated by the floating potential gradient, since this is much larger than the temperature gradient in the explored region. The magnetic field profile, reconstructed by the edge magnetic measurements, has been used to estimate the $\mathbf{E} \times \mathbf{B}$ flow. The diamagnetic term has been evaluated by the temperature and density profiles measured by Langmuir probes in the same discharges. Three points from spectroscopic measurements at the same plasma current are also shown in Fig. 1(b). The probe configuration allows a good spatial resolution in a region between the first wall and $r/a \sim 0.85$. On the other hand, spectroscopic measurements allow exploring the core region up to $r/a \sim 0.4$, although with a very poor spatial resolution. As can be observed, the measurements do not overlap, though the shapes of the profiles are similar: the spectroscopic velocity from CIII, at low plasma current, is lower by a factor of about three with respect to that measured by the probes. Since the electric field must be the same for all species, this difference could be due to the diamagnetic term in Eq. (1), because the details of the ion density and temperature profiles in the external region have substantial uncertainties for CIII (the diffusion model is not optimised to describe the very edge of the plasma).

3. Effect of external perturbations

3.1. Externally induced rotating magnetic perturbation

In RFX, the non-linear interaction among unstable $m = 0$ and $m = 1$ MHD modes causes their locking in phase and results in a localised helical deformation (LHD) of the plasma column. Experiments have been performed to drag the toroidal position of this LHD by an externally induced $m = 0$ magnetic perturbation [13]. The rotation velocity of the external perturbation is about 300 m/s, an order of magnitude lower than typical plasma rotation velocities. The CIII toroidal velocity has been found to be related to the instantaneous toroidal position of the perturbation, as shown in Fig. 2. As the perturbation toroidally approaches the diagnostic system, the CIII toroidal velocity changes from about −10 km/s, which is a typical value measured in discharges without rotating perturbation, to positive values. This effect is localised at the edge, because the inner CV rotation velocity is not affected by the toroidal position of the perturbation.

A similar behaviour is observed with Langmuir probes. As shown in Fig. 3, the edge electric field changes its direction (outward-directed) when the LHD is located at 217°, in correspondence to the probe

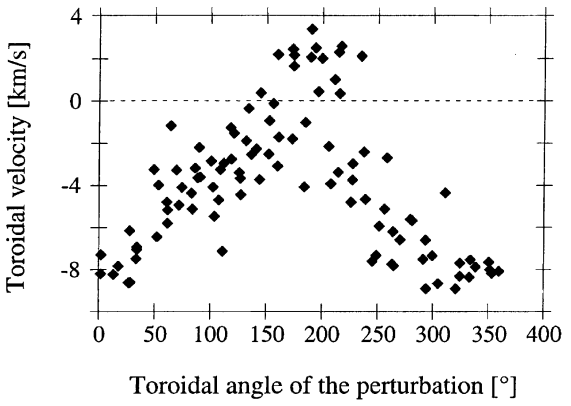

Fig. 2. CIII toroidal velocity as a function of the instantaneous toroidal position of the magnetic perturbation.

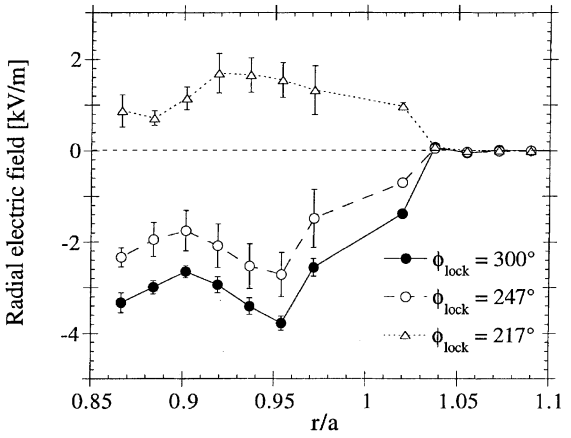

Fig. 3. Radial profile of the electric field measured by Langmuir probes as a function of the distance of the magnetic perturbation from the diagnostic position. The diagnostic is positioned at $\phi = 217°$.

toroidal position, while it is inward-directed when the perturbation is at 300°. If the LHD is interpreted as an outward deformation of the plasma column, as suggested by the associated large local horizontal shift of the plasma column (several centimetres), the modification of velocity and E_r might represent a more internal 'effective position' of the measurement in the plasma column.

3.2. Modification of E_r and plasma rotation by edge biasing

The radial electric field has been externally modified by means of two polarisable electrodes in 300 kA plasma current discharges. By negative biasing, E_r has been swept more negative in order to increase the $\mathbf{E} \times \mathbf{B}$ velocity and its shear and to reduce the particle flux driven by electrostatic turbulence [14]. The minimum value of $\mathbf{E} \times \mathbf{B}$ velocity at $r/a \sim 0.97$, deduced by electrostatic probe measurements, has been varied from −25 to −40 km/s. The velocity shear, $dv_{\mathbf{E}\times\mathbf{B}}/dr$, has been increased by a factor of two for $r/a > 0.92$ [14].

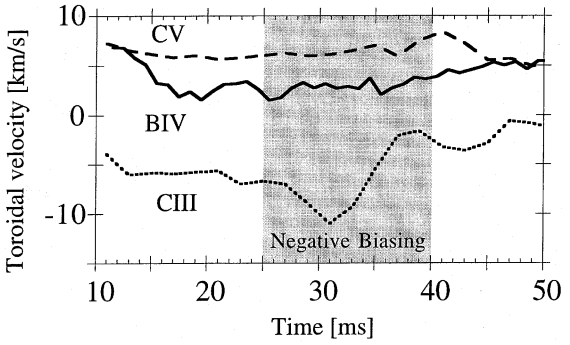

Fig. 4. Effect of negative edge biasing on CV, BIV and CIII toroidal velocities.

Spectroscopic measurements show that the edge velocity (CIII) is almost doubled during negative biasing (Fig. 4), while the other ions, associated with more internal radial positions, are not affected: this corresponds again to an increased velocity shear.

The positive biasing of the plasma results in an opposite effect: the CIII toroidal velocity decreases from its typical value between −6 and −10 km/s to about zero during the electrode action. Actually it has been experimentally observed that with positive edge biasing also $v_{\mathbf{E}\times\mathbf{B}}$ is reduced and sometimes inverts sign [15].

4. Interpretative models

A Monte Carlo model for the computation of the radial electric field in a self-consistent way has been developed [16,17]. The code considers an ensemble of test particles (hydrogen ions, carbon and oxygen impurities) moving inside the main plasma. It computes the main macroscopic quantities by averaging over this statistical ensemble. Test particles move in a fixed and known background of electron density and temperature, of neutrals hydrogen atoms and magnetic field. The macroscopic radial electric field is computed from the balance between the toroidal momentum lost by the plasma ions and the torque exerted by the return current [18]. Two sources of momentum loss are considered: direct losses due to ions impinging on the wall because of finite Larmor radius (FLR) effects and charge exchange losses due to ions being neutralised. The resulting electric fields show some features that are quite independent of the choice of the parameters: there are

two shear layers, in agreement with experimental data ([8], Fig. 1(b)), with a minimum negative value of E_r some mm inside the wall. The absolute value of the negative peak depends on the densities of electrons, impurities (which tend to increase it), and neutrals (E_r decreases with increasing neutrals).

The radial behaviour of plasma toroidal flow is also interpreted by applying a similar momentum balance equation in a single-fluid model, in analogy to what has been done in tokamaks [19], taking into account the viscosity and inertia terms. The equation has been written in cylindrical co-ordinates (r, θ, z) and solved in stationary conditions, assuming azimuthal and axial symmetry. The ion viscosity accounts for the total viscosity term and the dominant term in electron/ion collisions with neutrals is the ion-neutral charge exchange. The radial velocity v_r is taken as $D(1/n)(dn/dr)$, where n is the density and D is the anomalous particle diffusion coefficient. The axial component of the flow velocity, v_z, is obtained by numerically solving the balance equation written in [15] in terms of density and temperature and their first-order derivatives, and in terms of v_z and D and their first- and second-order derivatives. The boundary conditions are the experimental values of v_z at $r/a = 1$ and at the inner position. To take into account ion losses at the wall due to FLR effects, a force density term, F, has been added in the balance equation, with a radial profile $F = F_0 \exp[-((r/a - 1)/\sigma)^2]$, where σ corresponds to the width of the region where the return current is produced. This last quantity is computed using the previous Monte Carlo code. The result is compared with the value of v_z derived from the radial force balance using experimental data. The model has been applied to interpret the toroidal flow in standard discharges and in discharges modified by edge biasing.

Fig. 5 illustrates the toroidal component of the plasma velocity before ($J_{el} = 0$) and during negative edge biasing ($J_{el} = -160$ A m^{-2}), as obtained by electric probes in 300 kA discharges. Good agreement is found between the experimental values before edge biasing and the model, by imposing $F_0/B = -300$ A m^{-2} and $\sigma = 0.04$. This radial extension corresponds to 4–6 hydrogen Larmor radii and the value of F_0/B is of the same order of magnitude as the particle electrostatic flux measured in typical discharges. To simulate the toroidal flow in negatively polarised discharges, the value of F_0/B is set to 100 A m^{-2}, consistently with the observed reduction of the electrostatic particle flux during edge polarisation; the radial extension, σ, is unaffected. The radial profiles of temperature, density and diffusion coefficient have been changed in the calculation according to their modifications measured during the electrode action. It is worth noting that the internal shear layer is very well reproduced by the model; in this region, viscosity and inertial effects exceed friction with neutrals. The effect of positive biasing is foreseen by the model as well [15].

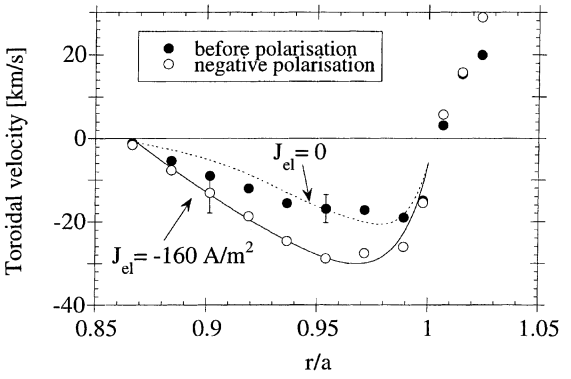

Fig. 5. Toroidal component of the plasma velocity before ($J_{el} = 0$) and during negative edge biasing ($J_{el} = -160$ A m^{-2}). The continuous and dotted lines are the single-fluid model simulations.

5. Summary and conclusions

The rotation velocity deduced from the Doppler shift of lines emitted by intrinsic impurities and from the electric and diamagnetic drift measured by electric probes has been discussed. In the external plasma region, $r/a > 0.8$, both diagnostics observe a toroidal rotation in direction opposite to the plasma current. Modifications of the plasma flow induced by external means such as $m = 0$ magnetic perturbation and polarisation with insertable electrodes have been also discussed.

The double shear structure of the electric field in proximity of the first wall has been reconstructed by a Monte Carlo simulation that considers the FLR losses and charge exchange losses as dominant terms in the momentum balance equation, while a single-fluid model allows a good simulation of the toroidal flow profile modified by edge biasing.

References

[1] K.H. Burrel, Phys. Plasmas 4 (1997) 1499.
[2] H. Biglari et al., Phys. Fluids B 2 (1990) 1.
[3] K.C. Shaing et al., Phys. Fluids B 2 (1990) 1492.
[4] B.A. Carreras et al., Phys. Fluids B 4 (1992) 3115.
[5] V. Antoni et al., Phys. Rev. Lett. 80 (1998) 4185.
[6] B.E. Chapman et al., Phys. Rev. Lett. 80 (1998) 2137.
[7] V. Antoni et al., Nucl. Fus. 36 (1996) 435.
[8] V. Antoni et al., Phys. Rev. Lett. 79 (1997) 4814.
[9] L. Carraro et al., Plasma Phys. Control. Fus. 40 (1998) 1021.
[10] L. Carraro et al., Plasma Phys. Control. Fus. 42 (2000) 1.
[11] A.B. Anton Rev. Sci. Instrum. 62 (1991) 832.

[12] V. Antoni et al., Nucl. Fus. 36 (1996) 435.
[13] R. Bartiromo et al., Phys. Rev. Lett. 83 (1999) 1779.
[14] V. Antoni et al., Plasma Phys. Control. Fus. 42 (2000) 83.
[15] D. Desideri et al., Czech. J. Phys. 49 (S3) (1999) 119.
[16] F. Sattin et al., in: Proceedings of the 25th EPS Conference on Controlled Fusion and Plasma Physics, Prague 1998, Mulhouse: EPS, paper B113PR, p. 778.
[17] V. Antoni et al., Experimental measurements and modelling of the structure of the radial electric field in RFX, Presented at the Third Europhysics Workshop on the Role of Electric Fields in Plasma Confinement and Exhaust, Budapest, 18–19 June 2000.
[18] R. Bartiromo, Phys. Plasmas 5 (1998) 3342.
[19] J. Cornelis et al., Nucl. Fus. 34 (1994) 171.